

Edyta BERNATOWSKA<sup>1</sup>  
Lucjan ŚLĘCZKA<sup>2</sup>

## STRESS AND STRAIN CONCENTRATIONS IN STEEL ANGLE TENSION MEMBERS CONNECTED BY ONE LEG

The paper presents the numerical simulations results of net section failure in tensioned angles. Angles are made of structural steel with nominal grade S235. Simulation takes into account ductile fracture initiation, by application of Gurson-Tvergaard-Needleman (GTN) material model. Parametrical analysis of ultimate resistance was carried out. The finite elements analyses were conducted by ABAQUS computer program. Shear lag effect in considered joint was observed, as a non uniform tensile stress distribution in angles in the vicinity of a connection. Stress concentration areas and stress concentration factors have been predicted, both in elastic and ultimate behaviour of joint. Especially change of non-uniform stress distribution in net cross-section was observed, during increase of loading, until the ultimate resistance was reached.

**Keywords:** lap bolted connections, shear lag effect, net section fracture, numerical simulations, stress and strain concentration

### 1. Introduction

Shear lag effect is a phenomenon of non-uniform stress distribution in wide flanges due to shear deformation [1]. In European code regulations it is practically equated with uneven distribution of normal stresses in wide flanges of plated structural elements in bending. The cause of the shear lag effect in such a case is the occurrence of shear deformation along the width of flanges in their mid-planes, per both sides of the web. This results in a non-linear distribution of normal stresses in the cross-section of the profiles, which is a deviation from the linear distribution, expected during bending in accordance with the Euler-

---

<sup>1</sup> Corresponding author: Edyta Bernatowska, Rzeszow University of Technology, The Faculty of Civil and Environmental Engineering and Architecture, Poznańska 2, 35-959 Rzeszów; +48178651629; e\_bernat@prz.edu.pl

<sup>2</sup> Lucjan Ślęczka, Rzeszow University of Technology, The Faculty of Civil and Environmental Engineering and Architecture, Poznańska 2, 35-959 Rzeszów; +48178651631; sleczka@prz.edu.pl

Bernoulli assumption “plane sections remain plan”. In analysis and limit states assessments it is taken into account by using a reduced “effective” flange width.

The second source of shear lag effect in steel structures, much more common than existing in plated structural elements in bending, are connections. In this case shear lag effect is defined as non uniform tensile stress distribution in a member or connecting element in the vicinity of a connection [2]. Such non uniform stress distribution is generally produced by applying force on the joint in local manner, when tension load is transmitted to some, but not all of the cross-sectional elements (where not all parts forming section are continuous in the joint).

Such way of constructing joints is very popular for practical reasons, eg. connecting I-shape only by web (by flanges), or connecting angle by only one leg is much more easier and cheaper compared to joints in which continuity of every part of element is provided (Fig. 1).

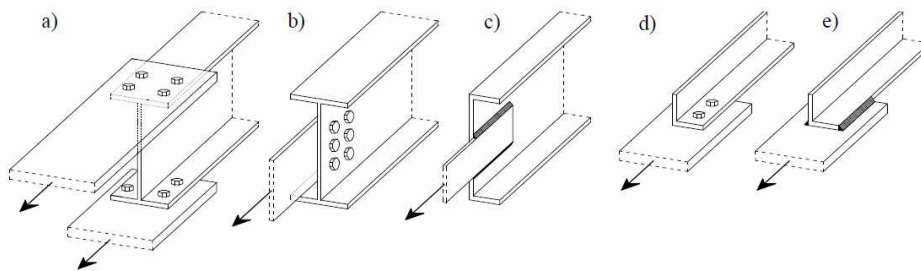


Fig. 1. Examples of joints in which shear lag effect occurs: a) I-section connected by flanges, b) I-section connected by web, c) C-section connected by web; d, e) angle connected by one leg using bolts or welds

In general case of connections, shear deformations are caused by introducing loads into a single part of cross section. In bolted shear connections stress distribution is also affected by existence of bolt holes, eccentricities and distributed pressure load in the bolt hole, close to net cross section, coming from bolt bear.

The shear lag effect in connections is known [3], [4] and included in design procedures [5], but there is a lack of detailed quantitative assessments of stress and strain concentrations which appear during gradual increase of loading. Areas of stress and strain concentration can influence the resistance of joint, where fracture of weakened cross section usually determines joint capacity. Especially value of stress concentrations factor in net cross-section can have an influence on ability of a material to deform plastically without losing its strength. The value of stress concentration can also influence initiation of fatigue crack in case of variable actions.

The paper presents a numerical simulation of net section failure of tensioned angles made of structural steel grade S235, connected by one bolt, with application of material model, taking into account ductile fracture initiation. Stress and strain concentrations areas both in elastic and ultimate behaviour of joint have been predicted as well as the stress concentration factors in elastic range. Also change of non-uniform stress distribution in net cross-section was observed, during increase of loading, until the ultimate resistance was reached.

## 2. Numerical simulations and comparison with test results

### 2.1. Range of analysis

The range of analysis covers ten equal leg angles connected by one bolt to the gusset plates, as is shown in Figure 2. The joints are made of two different sizes of angles, in each of them steel with nominal grade S235 was applied, where experimentally confirmed yield strength is equal to  $f_y=310$  MPa, and ultimate strength  $f_u=445$  MPa (using engineering stress measures). Bolts with diameters within the range from M18 to M22 were placed with different distance  $e_2$  from the edge. Bolts were fully threaded class 8.8. In the vicinity of the connection where the angle was supposed to rupture bolt hole was 2 mm larger than its diameter. Full description of analysed joints is given in Table 1.

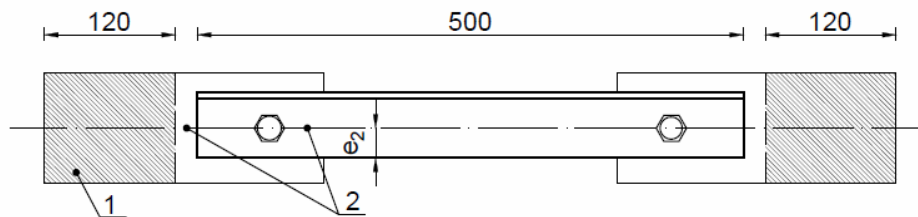


Fig. 2. Geometry of considered joints; 1) clamping area; 2) reference points to measure displacements

Table 1. Description of numerical models

Specimen	Cross-section	Bolt	Edge distance $e_2$ [mm]	Edge distance $e_1$ [mm]	$N_{FEA}$ [kN]	$N_{EXP}$ [kN]
J60/18/24	L60x6	M18	23.5	60.3	86.4	93.0
J60/20/27	L60x6	M20	25.6	65.1	87.8	83.8
J60/20/31	L60x6	M20	30.3	64.9	116.4	130.9
J60/22/27	L60x6	M22	25.5	74.0	93.4	105.6
J80/22/29	L80x6	M22	28.4	74.5	113.2	133.6
J80/22/32	L80x6	M22	30.7	74.3	122.4	132.1
J80/22/33*	L80x6	M22	33.0	74.3	131.0	-
J80/22/36	L80x6	M22	34.6	74.4	139.6	149.3
J80/22/37*	L80x6	M22	37.0	74.3	148.4	-
J80/22/39	L80x6	M22	38.9	74.3	157.5	177.6

## 2.2. Description of FE models

Finite elements models consisted of four element groups: angle, gusset plate, bolt with nut (modelled as a whole) and washers. The basis for the models were experimental tests, which are described in [6]. Generally ten specimens were analysed. Eight of them had exactly the same dimension as real specimens, two marked with asterisk (“\*”) were created for the needs of numerical investigation (see Table 1). Only half of the whole specimen was modelled, (Fig. 3).

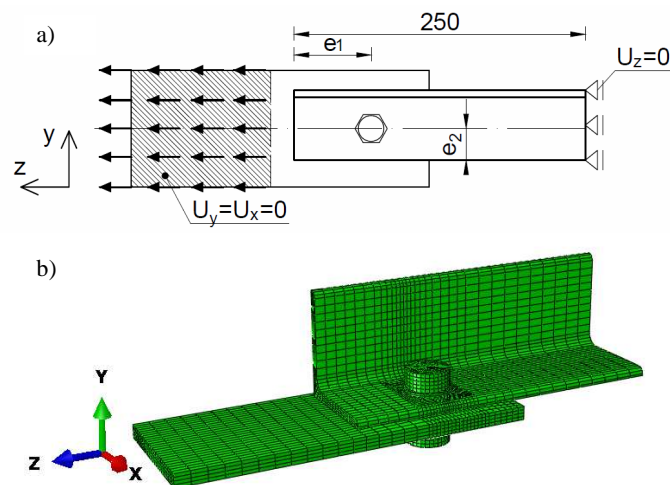


Fig. 3. Numerical models; a) schematic diagram; b) model made of finite elements

The load in  $z$ -direction has form of velocity, applied to the gusset plate. The hatched area (Fig. 3a) could not move in the direction of the  $x$  and  $y$  axes. The end of angle was blocked in  $z$ -direction. The bolt diameter was equal to the nominal value. Both washers and bolt were located concentrically with holes in angle and gusset plate.

The finite element mesh was adequately dense in the vicinity of the bolt hole in angle and gusset plate. The sides of cubic elements had similar length. Near the openings they were equal to 25% of angle thickness.

Elements of hierarchical validation were used during finite element modelling. At the beginning, choice of appropriate material model was made to simulate failure process of elements. Model's predictive capability was assessed by comparing calculations with experiments, what was described in publication [7].

Generally two types of material were implemented in models. For gusset plate, washers and bolt elastic-plastic material were used. Its behaviour was represented by a multi-linear stress-strain curve in terms of true stress and true plastic strain. They were evaluated from the standard tensile tests. The elastic behaviour was defined by Young's modulus and Poisson's ratio, equalling  $E = 210\,000$  MPa and  $\nu = 0.3$ .

For angles porous metal plasticity characteristics were introduced. This corresponds to the description of Gurson-Tvergaard-Needleman (GTN) material, which more properly controls the fracture process. Exact description of this material model can be found in [8]. Table 2 gives values of material parameters introduced to EF analysis.

Table 2. GTN material model parameter introduced to numerical simulation

$f_0$	Tvergaard parameters $q_i$	$f_N$	$\varepsilon_N$	$s_N$	$f_c$	$f_F$
0.001	$q_1=1.5; q_2=1.0; q_3=2.25$	0.02	0.3	0.1	0.06	0.2

For angles, gusset plates and washers C3D8R type of elements were employed. To apply a porous material in computer program, dynamic explicit analysis was chosen. Because of bolt pretensioning, which was modelled by means of temperature change in bolt shank, C3D8T and C3D6T elements were used. Relatively small clamping force was applied due to A category of joints according to EN 1993-1-8 [5].

Contact between components was defined using general contact option. The frictional effects between surfaces were included by incorporating the classical isotropic Coulomb friction model in the contact definition, with a friction coefficient  $\mu$  equal to 0.2.

### 2.3. Global results and observations

Global behaviour of joints, described by force-displacements curves, is shown in Figure 4. They are divided into two groups depending on angle size. Maximum values of resistance ultimate capacity obtained from FE modelling –  $N_{FEA}$  are slightly lower in most cases in comparison to those from test results –  $N_{EXP}$  (from 2% to 18%). Only in one specimen resistance obtained from FE modelling is 5% higher in comparison to the test (Table 1). Deformation capacity of joints, measured at two reference points (see Fig. 2), obtained from FE models is noticeably shorter when compared to real joints. But qualitative comparison of behaviour obtained from FE modelling to the one measured during the tests shows high degree of accuracy, especially in terms of deformations and fracture character, (Fig. 5). Detailed comparison FE results with tests is given in [7].

The edge distance  $e_2$  has the greatest impact on behaviour of modelled joints. The greater edge distance is, the greater resistance of specimens is observed. Looking at Table 1 and Figure 4, it can be seen that specimens J80/22/32 and J60/20/31 have almost the same edge distance  $e_2$ . Although they vary in angle and bolt size, they reached very similar tensile capacity and elongation.

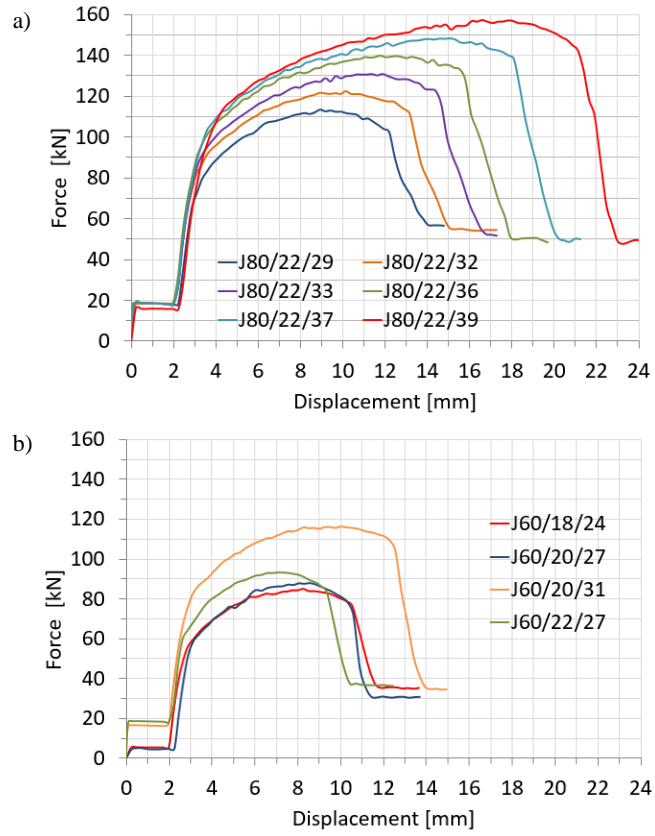


Fig. 4. Force - displacement curves from FE simulations; a) group made of L80x6, b) made of L60x6

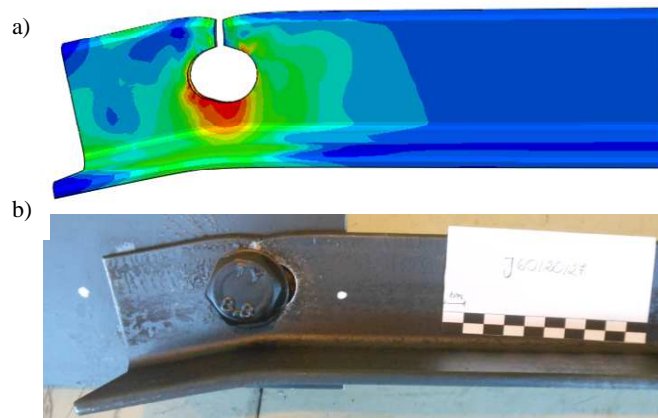


Fig. 5. Specimen J60/20/27; a) deformation and fracture mode obtained in FEA; b) obtained from test

It can be also observed that bolt diameter influences elongation of joints in a small extent. Specimens J60/20/27 and J60/22/27 (Fig. 4b) have the same edge distance  $e_2$  and they differ in bolt diameter. Ultimate resistance is slightly higher and elongation is smaller for specimen with larger bolts diameter despite the fact that net cross-section in this specimen is smaller.

### 3. Stress concentration factors in joints

One of the aims of this paper is to describe non-uniform stress distribution in net cross-section. Such description is possible so far only for welded angles and tees [9].

In elastic range the most convenient parameter which shows the stresses uniformity across considered element is the stress concentration factor  $k_t$ . Such factor is a ratio of maximum stress value to nominal ones. Within this work longitudinal stresses  $\sigma_{zz}$  were considered and nominal value of stress was calculated using tension force loading on angle and its net cross-section.

For all considered specimens stress concentration factors were calculated from equations (1) and (2).

$$k_t = \frac{\sigma_{max}}{\sigma_{nom}} \quad (1)$$

$$\sigma_{nom} = \frac{N}{A_{net}} \quad (2)$$

where:  $\sigma_{max}$  – maximum value of longitudinal stress ( $\sigma_{max} = \sigma_{zz}$ ) in steel angle,  
 $N$  – global force acting on joint equal to  $0.3N_{FEA}$ ,  
 $A_{net}$  – net cross-section.

The maximum values of longitudinal stresses were obtained from FE models for relatively small level of load (about 30% of  $N_{FEA}$ ), which on the one hand is greater from numerical slip resistance (Fig. 4), and on the other hand is enough small to longitudinal stress would be in elastic range of material characteristics.

For all specimens maximum values of  $\sigma_{zz}$  in elastic range appear in the vicinity of bolt hole (Fig. 6), not in net cross-section. So, two types of stress concentration factors were predicted. First one  $k_{t1}$  describes the largest value of concentration factor observed in specimen at all. Second one,  $k_{t2}$  describes stress concentration in net cross-section only, taking into account maximum stress in net cross-section.

Obtained values of  $k_{t1}$  and  $k_{t2}$  are given in the Table 3. It can be seen that difference between  $k_{t1}$  and  $k_{t2}$  changes in small extent (from 18 to 26%). Computed results of stress concentration factors are significantly larger compared with results for infinitive sheet in tension with circular hole, where  $k_t=3.0$  [10]. Obtained values are the results of additional bending caused by eccentricities and bearing stress created in the angle by the bolt.

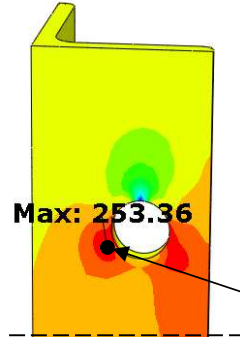


Fig. 6. Location of maximum value of  $\sigma_{zz}$  for J60/18/24 specimen

Table 3. Stress concentration factors

Specimen	$k_{t1}$	$k_{t2}$	$k_{t1}/k_{t2}$	$E_{FEA}$
J60/18/24	6.64	5.50	1.21	0.32
J60/20/27	5.86	4.74	1.24	0.35
J60/20/31	5.83	4.74	1.23	0.46
J60/22/27	5.08	4.03	1.26	0.37
J80/22/29	8.33	7.03	1.18	0.30
J80/22/32	6.86	5.78	1.19	0.33
J80/22/33	6.69	5.65	1.18	0.35
J80/22/36	6.33	5.33	1.19	0.37
J80/22/37	5.16	4.35	1.19	0.40
J80/22/39	5.16	4.35	1.19	0.42

To check correlation between predicted stress concentrations factors and ultimate resistance of joints additional parameter has been introduced. It is joint efficiency parameter  $E_{FEA}$ , which is defined as the ratio of finite element capacity (ultimate loading  $N_{FEA}$ ) over calculated nominal capacity of the net cross-section  $A_{net}$ :

$$E_{FEA} = \frac{N_{FEA}}{f_u A_{net}} \quad (3)$$

where:  $f_u$  – is ultimate strength of the steel.

Such joint efficiency parameter indicates cross-section utilization in tension members [9]. It can be observed that stress concentration factors  $k_{t1}$  and  $k_{t2}$  are inversely proportional to efficiency parameter  $E_{FEA}$ , especially in J80 group, in which edge distance  $e_1$  was constant. For this group also proportion  $k_{t1}/k_{t2}$  is nearly constant (1.18÷1.19).



#### 4. Process of stress redistribution under increasing load

Distribution of normal stress across the net cross-section in elastic range (Fig. 7) shows only area where yielding will start.

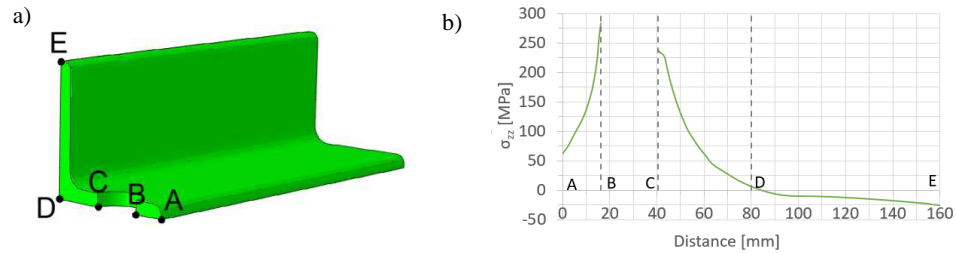


Fig. 7. Net cross-section; a) characteristic points, b) distribution of  $\sigma_{zz}$  in elastic range across net cross-section for specimen J80/22/29 for  $N=0.3N_{FEA}$

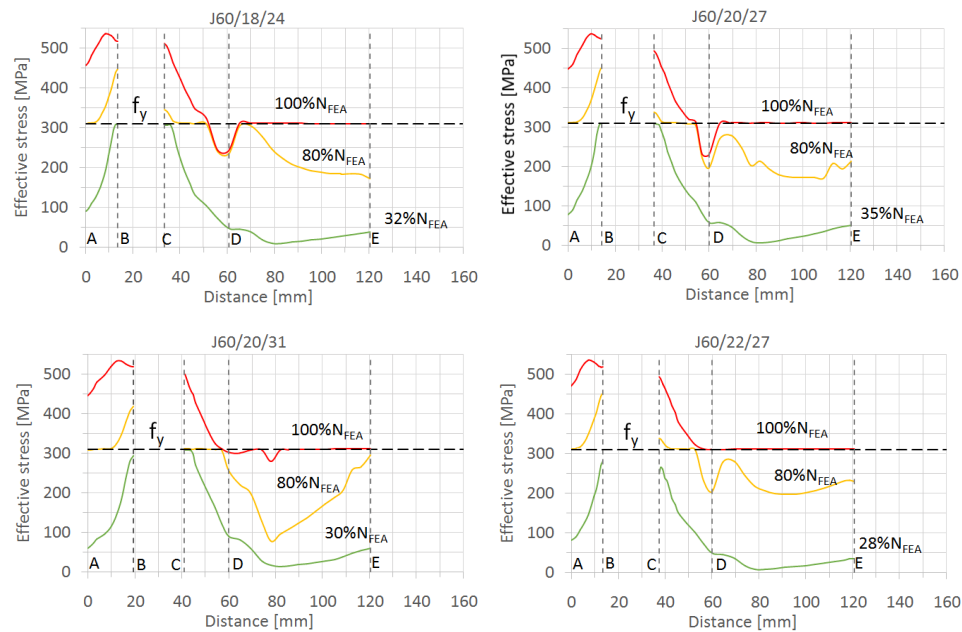


Fig. 8. Effective stress distribution in net cross-section (path A-E according to Fig. 7a) in three load levels, L60x6 angles

The change of stress distribution according to increasing level of loading is shown in Figure 8 and 9. Figures show distribution of effective stress along net cross-section (path which is defined in Fig. 7a) in three different load levels:

- $N=(0.28-0.35) N_{FEA}$ ,

- $N=0.80 N_{FEA}$ ,
- $N=N_{FEA}$ ,

where  $N_{FEA}$  is ultimate loading obtained in FE analysis.

Distance A-D refers to the width of connected leg, D-E to unconnected leg and B-C to the bolt hole.

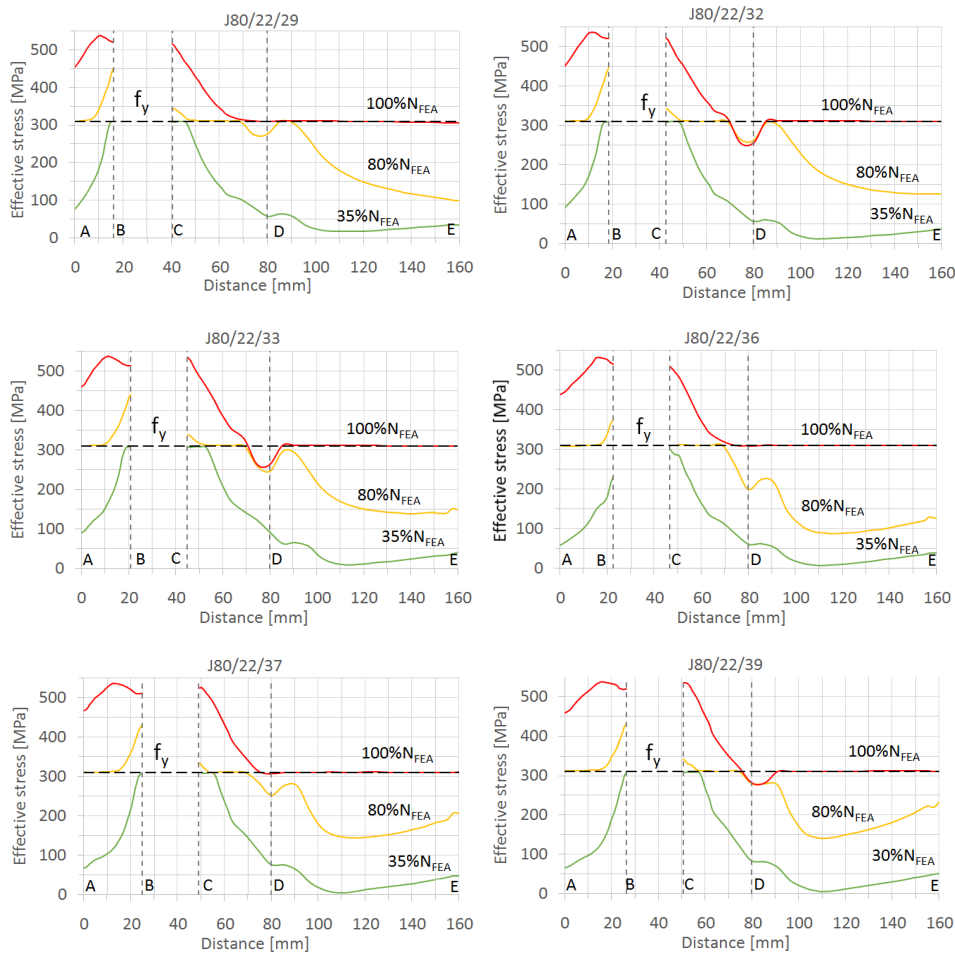


Fig. 9. Effective stress distribution in net cross-section (path A-E according to Fig. 7a) in three load levels, L80x6 angles

Presented diagrams were grouped according to the size of angles. They differ from each other in distance  $e_2$ . Dashed lines shows yield stress. To estimate effective stress, true stresses were used as a stress measures according to FE analysis type.

In all specimens it was observed that first material yielding started from area near the bolt hole in connected leg, and then spread over cross section. Stress in connected leg, in ultimate limit state, reached ultimate strength of steel, especially in section A-B in the vicinity of the bolt hole. Due to steel ductility, stress redistribution was observed before a final fracture, allowing yielding of unconnected leg D-E. However effective stress value across unconnected leg of angle does not exceed yield strength of the steel.

The sequence of initiation and propagation of fracture obtained during FE analyses was the same as during the test. Fracture initiation occurs with significant plastic deformation of the connected leg fragment, between bolt hole and adjacent edge. Concentration of longitudinal true strain  $\epsilon_{zz}$  is observed on the bolt hole edge (Fig. 10).

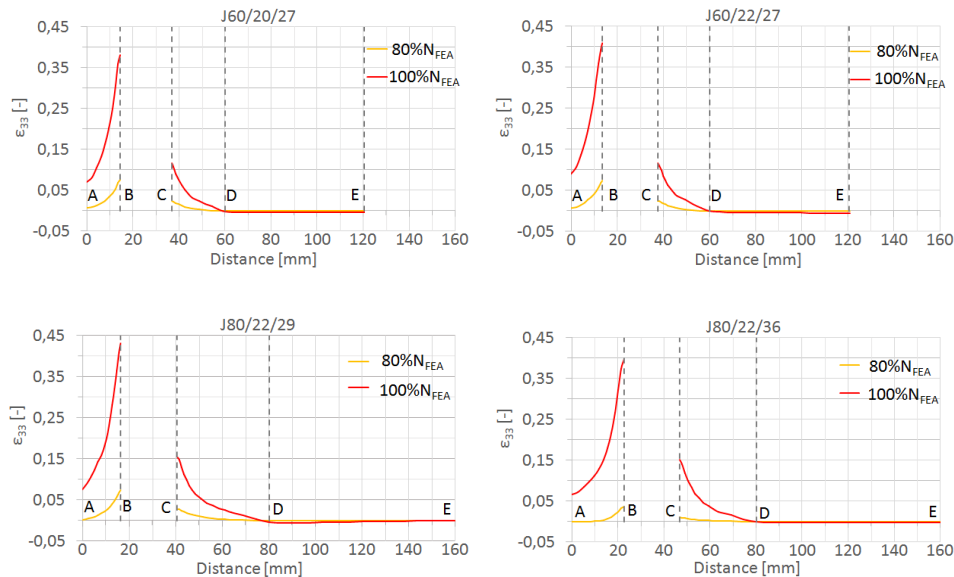


Fig. 10. True strain  $\epsilon_{zz}$  distribution in net cross-section (path A-E according to Fig. 7a) in two loading levels in selected specimens

## 5. Summary and conclusion

Results of numerical investigation on the shear lag effect of steel tension angles, connected by one bolt, are reported in this paper.

Conducted analyses show non uniform tensile stress distribution in angles, in the vicinity of a connection, both in elastic range and at the stage of reaching the ultimate load capacity. In elastic range stress concentration factors predicted for analyzed joints have clearly larger values than in other bolted lap connections.

Ductile nature of structural steel can lead to total yielding of net cross-section, but in order to obtain ultimate resistance of net cross-section, only part of connected leg area is utilized.

Analyses gave better insight into process of redistribution of stress along net cross section during increasing loading, which can be use in further work.

## References

- [1] EN 1993-1-1 Eurocode 3: Design of steel structures – Part 1-1: General rules and rules for buildings. European Committee for Standardization, Brussels, 2005.
- [2] ANSI/AISC 360-10 An American National Standard. Specification for Structural Steel Buildings. American Institute of Steel Construction, 2010.
- [3] Kulak G.L., Wu Y.: Shear lag in bolted angle tension members, *Journal of Structural Engineering*, vol. 123(9), 1997, pp. 1144–1152.
- [4] Može P.: Angles connected by one leg in tension, Eurosteel 2017, September 13-15, 2017, Copenhagen, Denmark, [onlinelibrary.wiley.com/doi/10.1002/cepa.433](https://onlinelibrary.wiley.com/doi/10.1002/cepa.433).
- [5] EN 1993-1-8 Eurocode 3: Design of steel structures – Part 1-8: Design of joints, European Committee for Standardization, Brussels, 2005.
- [6] Błyskal E., Ślęczka L.: Experimental tests of angle tension members connected by one bolt (in Polish), *Czasopismo Inżynierii Lądowej, Środowiska i Architektury – Journal of Civil Engineering, Environment and Architecture, JCEEA*; t. XXXIII, z. 63 (1/I/16), 2016, pp. 323–330, DOI:10.7862/rb.2016.38.
- [7] Bernatowska E., Ślęczka L.: Net section fracture assessment of steel bolted joints with shear lag effect. 64 Konferencja Naukowa KILiW PAN oraz KN PZITB, Krynica 2018 (paper accepted for publication).
- [8] Kossakowski P.: Application of damage mechanics in the analysis of pre-failure states of metal structures (in Polish), *Zeszyty Naukowe Politechniki Rzeszowskiej Budownictwo i Inżynieria Środowiska*, no. 59 (3/12/II), 2012, pp. 177–184.
- [9] Fang Ch., Lam A.C.C., Yam M.C.H.: Influence of shear lag on ultimate tensile capacity of angles and tees. *Journal of Constructional Steel Research* 84 (2013) pp. 49–61.
- [10] Schijve J.: *Fatigue of structures and materials*. Springer 2009.

*Przesłano do redakcji: 01.05.2018 r.*

*Przyjęto do druku: 15.06.2018 r.*